

# Laser Ablation of Mg Metal Target under Copper Vapor Laser in Acetone Liquid Medium

Fahimeh Abrinaei\*

Department of Physics, East Tehran Branch, Islamic Azad University, Tehran, Iran

## Abstract

A homemade Copper Vapor Laser (CVL) operating at 510 nm (green) and 578 nm (yellow) outputs was applied to vaporize the Mg metal target in the acetone liquid medium. The Mg plate surface was ablated under a 10 kHz repetition rate and maximum pulse energy of 3 mJ and 35 ns pulse duration. Structural, morphological, optical, and chemical-bond properties of synthesized Mg and MgO nanoparticles were investigated using the X-ray diffraction (XRD) analysis; scanning electron microscopy (SEM) observations, UV-VIS absorption spectroscopy and Fourier transform infrared spectroscopy (FTIR) analysis, respectively. The XRD results confirmed the formation of both Mg and MgO nanoparticles. The crystallite size and the strain of final powder were estimated about 57 nm and 0.017 from XRD data calculated using the Williamson-Hall method. The Mg/MgO ratio was also calculated to be about 67% according to Alexander & Klug formula. The chemical bands of products were correctly identified using the FTIR characterization. The SEM images revealed the presence of spherical and platelet-like structures in a range of 50-80 nm in diameter that confirmed the XRD results. UV-VIS absorption spectrum of Mg/MgO nanoparticles synthesized by laser ablation of Mg target in acetone shows a broad peak at about 417 nm attributed to the plasmon absorption band at this wavelength. The derivative method was applied to measure the  $E_g$  equal to 2.3 eV for Mg/MgO nanoparticles synthesized in acetone medium under CVL ablation.

**Keyword:** Magnesium (Mg) • Magnesium Oxide (MgO) • Copper Vapor

## Introduction

Easy and cost-effective synthesis process, high chemical and thermal stability, availability, and non-toxicity are important factors regarding the selection of materials and methods to synthesize the nanostructured materials. Laser ablation methods as an attractive technique for preparation of nanoparticles and nanomaterial have been the focus of attention since the discovery of nanotechnology science. Considerable interest in laser processing nanomaterials in liquids is due not only to the ability to control the compositions, particle size, production rate and morphology of the ablated product by a tailored selection of liquid medium, surfactants and other additives but also for easy and cost-effective synthesis process due to the lack of need for vacuum protection.

Magnesium (Mg) and magnesium oxide (MgO) nanoparticles have attracted a lot of attention in recent years. Magnesium oxide is an excellent candidate for chemical industry applications as a scrubber for air pollutant gases (CO<sub>2</sub>, NO<sub>x</sub>, SO<sub>x</sub>) and as catalyst support. MgO is an important inorganic material that possesses a wide band gap energy ( $E_g \sim 7.8$  eV) [1]. MgO nanostructures are used in pharmaceutical and medicinal chemistry, in which the treatment of diseases such as tumor search and other cases are generally

considered [2]. MgO nanoparticles are an antibacterial agent with the advantages of being nontoxic and relatively easy to obtain [3]. MgO nanostructures have drawn special attention because of their important applications in the areas of catalysis, refractory materials, and superconductors. MgO nanoparticles can be applied in electronics, catalysis, ceramics, petrochemical products, coatings and many other fields. MgO nanoparticles can be used along with wood chips and shavings to make materials such as sound-proof, light-weight, heat-insulating, and refractory fiberboard and metallic ceramics.

Mg is widely used as an excellent candidate for weight critical structural applications because of its impressively low mass density that renders a high specific stiffness and strength. It also possesses good dimensional stability, high damping capacity and good high temperature creep properties [4, 5]. Phuoc et al. synthesized Mg/MgO nanocrystallites by laser ablation of Mg in acetone and isopropanol with a Q-switched Nd-YAG laser operating at 1064 nm and investigated structural properties of the formed Mg/MgO nanostructures [6]. Abrinaei et al. reported on the study of structural properties of Mg/MgO nanoparticles synthesized by Nd-YAG ( $\lambda = 1064$  nm) laser as well as CVL (Cooper Vapor Laser) in isopropanol [7].

\*Address for Correspondence: Fahimeh Abrinaei, Department of Physics, East Tehran Branch, Islamic Azad University, Tehran, Iran; E-mail: f\_abrinaey@yahoo.com; Tel: +989193117542

Copyright: © 2022 Abrinaei F. This is an open-access article distributed under the terms of the creative commons attribution license which permits unrestricted use, distribution and reproduction in any medium, provided the original author and source are credited.

Received: 19-Jun-2020, Manuscript No. JLOP-22-001; Editor assigned: 23-Jun-2020, Pre QC No. JLOP-22-001 (PQ); Reviewed: 24-Jul-2020, QC No. JLOP-22-001; Revised: 28-Sep-2020, Manuscript No. JLOP-22-001 (R); Published: 04-Aug-2022, DOI: 10.37421/2469-410X.22.9.226

A series of experiments are presented here. These experiments are performed on the formation of Mg & MgO nanostructures by copper vapor laser (CVL) ablation of a magnesium target in acetone liquid medium and investigation of structural, morphological, optical, and chemical-bond properties of synthesized Mg and MgO nanoparticles. A CVL operating at 510 nm (green) and 578 nm (yellow) outputs were used to ablate Mg target in acetone (CH<sub>3</sub>COCH<sub>3</sub>), so that Mg and MgO nanoparticles were synthesized and characterized by XRD, UV-VIS, SEM, and FTIR analyzes.

### Methodology synthesis

Mg/MgO nanoparticles were prepared by laser ablation of Mg metal plate (99.99%) in acetone. As shown in Fig. 1, the target was put at the bottom of a glass vessel filled with 5 ml acetone. The laser beam was focused on the surface of the magnesium target. The liquid depth above the target surface was several millimeters. An ablation setup was provided for the about 3 mJ/pulse of CVL (wavelength: 510 nm, green and 578 nm yellow, FWHM: 35 ns, repetition rate: 10 kHz) laser. The laser ablation process lasted for 60 min. During the ablation in acetone, the spark plumes become larger with a cracking noise. Small bubbles were observed and suggest that acetone was pyrolyzed during the laser ablation process. Upon irradiation of the laser beam, the color of the solution turned light metallic gray. Structures were not stable and the rapid agglomeration even pending the laser ablation process. These agglomerations precipitated at the bottom of the container, rapidly.

### Characterization

After laser ablation, a small amount of colloidal solution was transferred into a quartz cell for UV-VIS spectroscopy analysis. The optical absorbance of the sample was measured by using a high-resolution spectrophotometer, Camspec, ModelM350 in the wavelength range of 200-1000 nm.

X-ray diffraction patterns of structures were recorded by evaporation of the colloidal solutions onto a glass substrate at room temperature (Fig. 1). The crystal structure of the sample was analyzed by a Philips diffractometer (STADI MP) with Cu K $\alpha$  radiation, angle step size of 0.02 $\theta$ , and count time of 1.0 second per step.

An amount of wet precipitate was transferred to a quartz vessel placed in the open air to evaporate the liquid to acquire some powder for FTIR investigations (Figure 1). The FTIR spectrum is prepared by a Thermo Nicolet NEXUS 870 FT\_IR model spectrophotometer.

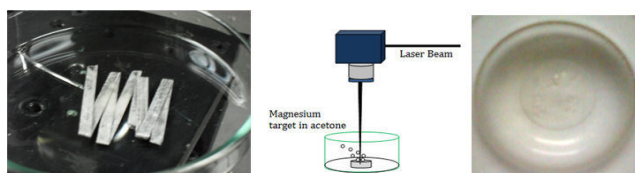


**Figure 1** From left to right: magnesium tape in acetone before ablation; a schematic diagram of the laser ablation setup; the sedimentation of the final product.

Some drops of Mg/MgO colloidal solution have also been deposited onto an Aluminum plate to perform SEM analysis with a TS5136MM microscope operating at 30 kV.

## Results and Discussion

### XRD analysis

The phase and crystallographic structure can be identified by the XRD pattern of the structures prepared by CVL ablation of magnesium target in acetone in Figure 2. The XRD pattern indicates that both MgO and Mg are presented in the sample with a higher percentage of Mg. It is clear from the XRD pattern that the prepared powders are polycrystalline structures inclusive Mg and MgO. The weight percentage of each Mg and MgO nanoparticles can be calculated by Rietveld method [8]. The Mg/MgO ratio in the final product synthesized by laser ablation of magnesium target in acetone was calculated at about 67/33 percentage.

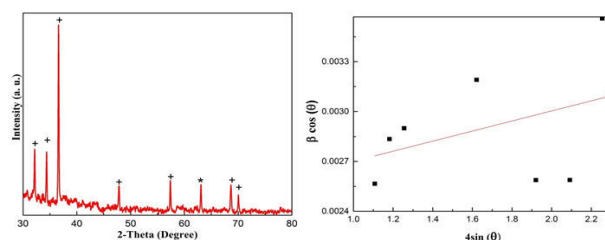


**Figure 2** XRD pattern and Williamson-Hall plot of Mg/MgO nanoparticles synthesized by laser ablation method under CVL in acetone. Note: (+) Mg; (\*)MgO

To estimate the crystallite size and the strain of Mg/MgO nanoparticles, the Williamson-Hall method was applied using the following equation [9]:

$$\beta \cos\theta = 0.9\lambda/D + 4\varepsilon \sin\theta \quad (1)$$

Where D is average crystallite size in nm,  $\lambda$  is the wavelength of X-ray source (0.154 nm),  $\beta$  (in radian) is full width at half maximum of the peaks and  $\varepsilon$  is the strain of lattice. The strain and average crystallite size values can be estimated by plotting the  $\beta \cos\theta$  against  $4\sin\theta$  to get a straight line with slope  $\varepsilon$  and intercept  $0.9\lambda/D$ . The values of strain and crystallite size of Mg/MgO nanoparticles deduced from X-ray diffraction calculations according to the Williamson-Hall method are estimated about 0.017 and 57 nm, respectively.

### Optical properties

Figure 3 shows the UV-VIS optical absorption spectrum of the colloidal suspension of the sample in acetone. As can be observed in Figure 3, there is a characteristic absorption band at about 417 nm.

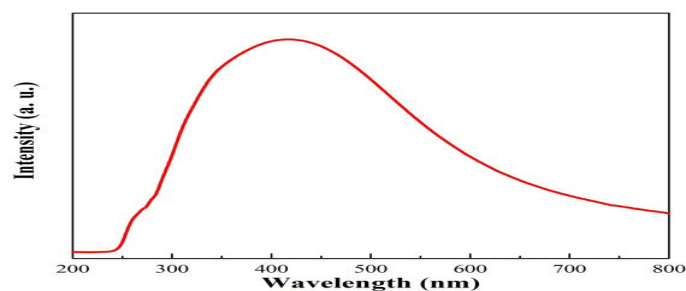


**Figure 3** UV-VIS spectrum of Mg/MgO nanoparticles prepared by CVL ablation of magnesium target in acetone.

The measurement of the energy bandgap,  $E_g$ , is important in the micro- and nano-materials. There are various methods for calculation

of Eg. In this work, the energy bandgap was determined using UV-Vis absorption spectrum of Mg/MgO nanoparticles. The derivative method was applied for the measurement of Eg. In this method, the first derivative of the absorbance was evaluated near the fundamental absorption edge, leading to Eg [10]. The energy bandgap value is obtained equal to 2.3 eV for Mg/MgO nanoparticles.

The calculated bandgap of Mg/MgO nanoparticles synthesized by laser ablation method in acetone is significantly smaller than the wide bandgap energy 7.8 eV expected for the bulk, pure, crystalline MgO. Therefore, it is clear that Mg/MgO nanoparticles have metallic conduction behavior [11].

FTIR transmittance spectrum in the wavenumber range of 4000–500  $\text{cm}^{-1}$  for the Mg/MgO nanoparticles produced by laser ablation of Mg in acetone is presented in Figure 4.

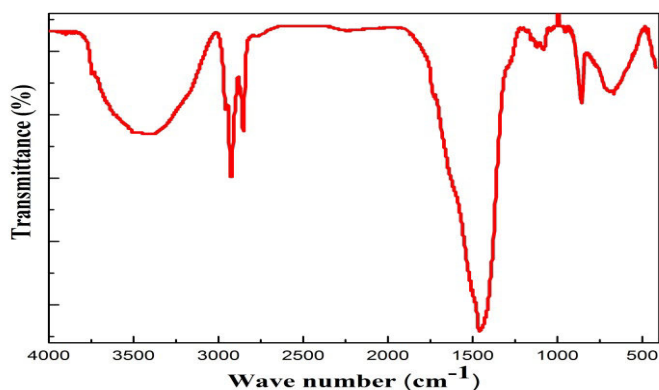


**Figure 4** FTIR spectrum of Mg/MgO powder prepared by laser ablation of Mg target in acetone.

In the FTIR spectrum, the stretching bands of the superficial OH groups are seen in the region between 4000 and 3500  $\text{cm}^{-1}$ . The absorption band around 3448  $\text{cm}^{-1}$  is broad and corresponds to the –OH-group-stretching vibration that is dedicated to –OH-stretching mode of residue water and absorbed acetone on the surface of Mg/MgO nanoparticles. This peak shows the presence of the hydroxyl group at low coordination sites or defects [12]. The absorption bands around 2926 and 2851  $\text{cm}^{-1}$  are due to surface OH stretch appearing from hydroxyl groups in dissociated state or C–H stretch of organic residue [13], where these peaks are due to surface OH stretch in-phase and out of phase, respectively. The peak at 1672  $\text{cm}^{-1}$  was attributed to the bending vibration of the water molecule. An absorption peak at 1457  $\text{cm}^{-1}$  is assigned to  $\nu_a(\text{C}-\text{O}) + \delta(\text{O}=\text{C}-\text{O})$  modes. Thus, these contain signatures of adsorption and chemisorption of water and acetone. Two sharp absorption peaks at 1107 and 970  $\text{cm}^{-1}$  are devoted to C–O/C–O stretching modes. While the band at 861  $\text{cm}^{-1}$  corresponds to  $\nu(\text{Mg}-\text{O}) + \delta(\text{O}-\text{C}=\text{O})$ , a peak at 673  $\text{cm}^{-1}$  is ascribed to the bending mode of O=C=O or vibration of water. The two peaks at 450  $\text{cm}^{-1}$  and 515  $\text{cm}^{-1}$  affirmed the presence of Mg–O vibrations [14, 15].

### Morphological properties

SEM image of Mg/MgO nanoparticles synthesized by CVL ablation of magnesium target in acetone (Figure 5).

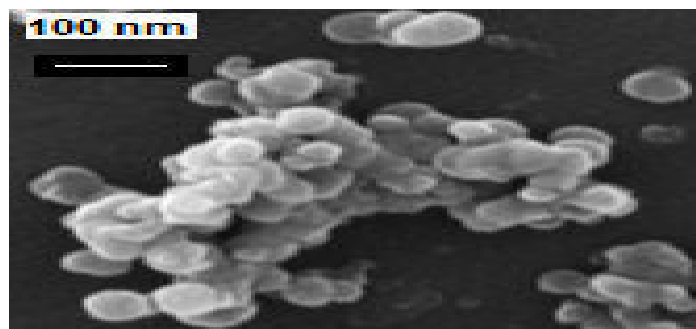


**Figure 5** SEM image of Mg/MgO nanoparticles synthesized by CVL ablation of magnesium target in acetone.

The SEM image reveals that the Mg/MgO nanoparticles are constructed of particles with the nearly spherical and platelet-like shapes in a range of 50–80 nm that confirmed the XRD results.

### Conclusion

Laser ablation of magnesium in acetone has been conducted in this study. The XRD spectrum showed that MgO and Mg nanoparticles have been formed. The ablation of magnesium in acetone yielded spherical and plate-like structures having an average size of 50–80 nm. UV-VIS spectrum indicated a characteristic absorption band at about 417 nm. The energy bandgap of Mg/MgO nanoparticles calculated equal to 2.3 eV.

### References

1. Gaashani, RA., Radiman S, Douri Y and Tabet N, et al. Investigation of the optical properties of Mg(OH)<sub>2</sub> and MgO nanostructures obtained by microwave-assisted methods. *J Alloy Compd.* 52 (2012):76
2. Di, DR., He ZZ, Sun, ZQ and Liu J. A new nano-cryosurgical modality for tumor treatment using biodegradable MgO nanoparticles. *Nanomed.* 8(2012): 1233-1241.
3. Tang, ZX. and Lv BF. MgO nanoparticles as antibacterial agent: preparation and activity. *Braz. J Chem Eng.* 31(3), 591-601 (2014).
4. Ferkel, and BL Mordike. Magnesium strengthened by SiC nanoparticles. *Mater Sci Eng .A*, 193 (2001).
5. SF, Hassan and M Gupta.. Fabrication of TiB<sub>2</sub> particulate reinforced magnesium matrix composites by two-step processing method. *Mater Sci Technol.* 19 (2003): 249-253.
6. Phuoc, TX., Howard BH, Martello DV and Soong Y, et al. Synthesis of Mg(OH)<sub>2</sub>, MgO, and Mg nanoparticles using laser ablation of magnesium in water and solvents. *Opt Laser Eng.* 46 (2008): 829-834.
7. Abrinaei, F., Torkamany MJ, Hantezadeh MR and Sabbaghzadeh J. Formation of Mg and MgO nanocrystals by laser ablation in liquid: effects of laser sources. *Sci Adv Mater.* 4 (2012):501-506.
8. Snellings, R., Machiels L, Mertens G and Elsen J. Rietveld refinement strategy for quantitative phase analysis of partially amorphous zeolitised tuffaceous rocks. *Geologica Belgica.* 13(2010): 183-196.
9. GK Williamson and WH Hall. Radiation effects in nuclear waste forms for high-level radioactive waste. *Acta Metall.* 1 (1953) 22-29.
10. Ferreirada, Silva., Veissid NA, An CY and Pepe I, et al. Optical determination of the direct bandgap energy of lead iodide crystals. *Appl Phys Lett.* 69(1996): 1930-1932.

11. Kurth, M., Graat PCJ and Mittemeijer EJ. The oxidation kinetics of magnesium at low temperatures and low oxygen partial pressures. *Thin Solid Films* 500 (2006): 61-69.
12. Site, LD and Alavi A. Lynden-Bell RM. Structure and spectroscopy of a monolayer of water on MgO (100). *J Chem. Phys.* 113 (2000): 3344-3350.
13. Rezaei, M and Khajenoori M. Nematollahi B. Synthesis of high surface area nanocrystalline MgO by pluronic P123 triblock copolymer surfactant. *Powder Technol.* 205(2011): 112-116.
14. Alavi, MA and Morsali A. Syntheses and characterization of Mg(OH)<sub>2</sub> and MgO nanostructures by ultrasonic method. *Ultrason Sonochem.* 17(2010): 441-446.
15. Ganeev, RA and Usmanov T. Nonlinear-optical parameters of various media. *Quantum Electron.* 37(2007): 605-622.

**How to cite this article:** Abrinaei, Fahimeh, "Laser Ablation of Mg Metal Target under Copper Vapor Laser in Acetone Liquid Medium" *Laser Opt Photonics* 9 (2022): 267.